Closed-loop Control of Functional Neuromuscular Stimulation

NIH Neuroprosthesis Program Contract Number N01-NS-6-2338
Quarterly Progress Report #5
April 1, 1997 to June 30, 1997

Investigators:
Patrick E. Crago, Ph.D.
Clayton L. Van Doren, Ph.D.
Warren M. Grill, Ph.D.
Michael W. Keith, M.D.
Kevin L. Kilgore, Ph.D.
Joseph M. Mansour, Ph.D.
P. Hunter Peckham, Ph.D.
David L. Wilson, Ph.D.

Departments of
Biomedical Engineering,
Mechanical and Aerospace Engineering,
and Orthopaedics
Case Western Reserve University
and MetroHealth Medical Center

This QPR is being sent to you before it has been reviewed by the staff of the Neural Prosthesis Program.

Table of Contents

1. SYNTHESIS OF UPPER EXTREMITY FUNCTION

The overall goals of this project are (1) to measure the biomechanical properties of the neuroprosthesis user's upper extremity and incorporate those measurements into a complete model with robust predictive capability, and (2) to use the predictions of the model to improve the grasp output of the hand neuroprosthesis for individual users.

1. a. BIOMECHANICAL MODELING: PARAMETERIZATION AND VALIDATION

Purpose

In this section of the contract, we will develop methods for obtaining biomechanical data from individual persons. Individualized data will form the basis for model-assisted implementation of upper extremity FNS. Using individualized biomechanical models, specific treatment procedures will be evaluated for individuals The person-specific parameters of interest are tendon moment arms and lines of action, passive moments, and maximum active joint moments. Passive moments will be decomposed into components arising from stiffness inherent to a joint and from passive stretching of muscle-tendon units that cross one or more joints.

Report of progress

1. a. i. MOMENT ARMS VIA MAGNETIC RESONANCE IMAGING

Abstract

In this quarter, a program was created to extract useful, 2D slices from a three dimensional image volume. This program is useful for visualization of joint motion as well as for measurement of tendon moment arm using a 2D geometric method. We also implemented a 2D geometric method to measure the tendon moment arm that used the method of Realeaux to find the axis of rotation. We continued imaging experiments on more subjects. In the next quarter, we will be testing this 2D method and compare the results with that of the other two 3D methods on a larger set of image data.

Progress Report

As described previously, we are testing methods for measuring tendon moment arm in the MCP joints of the fingers. We consider this joint to be simpler than the wrist; hence, we elect to study it first. We use high-resolution, 3D MRI to measure tendon moment arm, and our initial goal is to determine an accurate, practical method. As described in the proposal, we are examining 3 methods for analyzing tendon moment arm. They are: tendon excursion, 3D geometric, and 2D geometric. In previous reports, we detailed the tendon excursion and the 3D geometric method. In this report, we describe the 2D geometric method.

It is difficult to extract a single, thin image slice showing the length of the tendon as well as the two bones comprising the third MCP joint, and we created a computer program especially for this purpose. The technique is to identify three markers in the 3D image set. Two of the three markers are on the third metacarpal bone and the other marker is on the third phalanx. These three points define a plane, and a single, reformatted slice from the volume. Within this single slice, one can clearly see the tendon and bones. This process is repeated for each image data volume using the same 3 markers. This program greatly aids visualization of tendon and bone motion during flexion. It is also used to measure tendon moment arms using the 2D geometric method described next.

We have also implemented a 2D geometric method for measuring the tendon moment from the extracted slice images. This method is very similar to a method proposed by Rugg et al. (Biomechanics, 23:495-501, 1990). Rather than the manual method of Rugg, we use a computer program where the operator chooses 4 points of interest, two on each bone, in each slice image taken at different joint rotation angles. From these (x,y) points, the center of rotation is obtained. The moment arm is the distance between the center of rotation to the tendon center line. We use a single slice 1 mm thick whereas Rugg et al. used a 10 mm thick slice for the ankle. A thin slice will reduce image spatial averaging and give more accurate results.

We have used this 2D geometric method to measure moment arms on the flexor digitorum profundus tendon of two subjects. Preliminary indications are that this method is not as repeatable as the other, 3D methods.

In this period, we have performed several imaging experiments. We now have imaged a total of 4 subjects, each measured on two days. We are in the process of analyzing these data.

Plans for next quarter

We will compare and analyze the results of the 3 methods over multiple subjects and imaging sessions. We will compare moment arm values, repeatability, image acquisition time, analysis time, etc. We will also compare inter-observer variability of the analysis methods. At the end of this study, we should know better what methods to apply to patients.

1.a.ii. PASSIVE AND ACTIVE MOMENTS

Abstract

This report includes an analysis of the normal variation in the computed moment angle curve (MAC) parameters over time. Data that were collected at different times post surgery were analyzed to determine how the passive properties of a neuroprosthesis user changes over time. Finally, an example case is presented to show how the methods of analysis developed in this study can be used to predict the cause of joint passive property disorders.

Purpose

The purpose of this project is to characterize the passive properties of normal and paralyzed hands. This information will be used to determine methods of improving hand grasp and hand posture in FES systems.

Report of Progress

Normal Variation in MAC Parameters Over Time

It is important to be able to quantify changes in the joint condition that may be occurring as a result of treatment. Such information can be used to determine if the treatment is helping the condition or not and if it should be continued or stopped. If no treatment is being given, monitoring the passive properties of a joint over time can provide information that indicates whether the condition is improving on its own or getting worse.

In order to properly evaluate the effects of a given treatment on the passive properties of a joint over time, it is first necessary to know how the passive properties of a normal joint vary over time. To test the normal variability in the passive moment, one able bodied subject's MP joint was tested six times at random intervals over a period of 16 days. Figure 1.a.ii.1 shows all six MACs plotted on the same axes. The rest position, extension and flexion limits, extension and flexion stiffnesses, and PROM were computed for each MAC. The maximum, minimum, range, and coefficient of variation for each of these parameters are shown in Table 1.a.ii.1. The rest position and stiffness parameters varied the most from day to day. For a change in a given MAC parameter to be attributed to a certain treatment, the parameter should have changed with a magnitude greater than the range shown for that parameter in Table 1.a.ii.1.

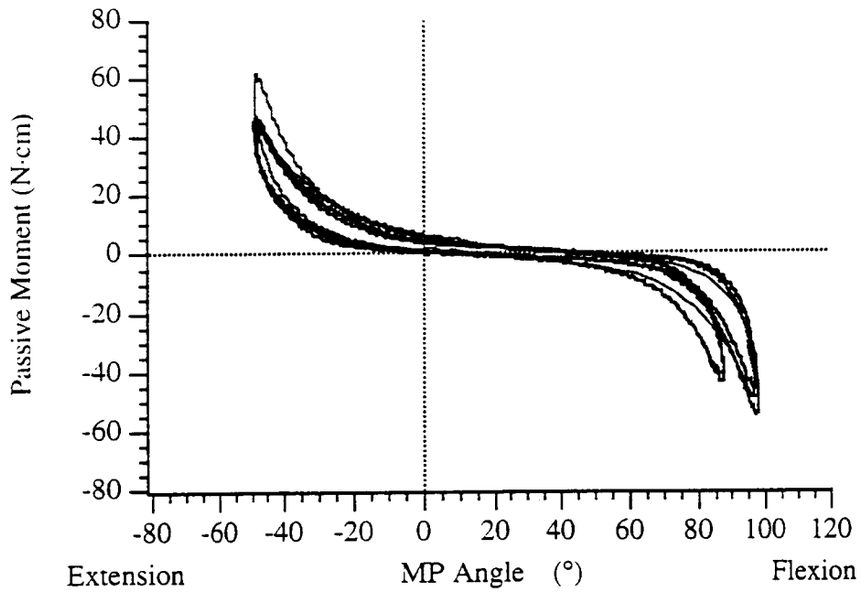

Figure 1.a.ii.1. Plot showing the variation in the moment angle curves measured from a single joint over a period of 16 days.

Table 1.a.ii.1. Day to Day Variability in the MAC Parameters

MAC Parameter	*Max.*	*Min.*	*Range*	*Coeff. of Var. (%)*
Passive Range of Motion (°)	127	114	13	3.9
Extension Limit (°)	-39	-35	4	4.3
Flexion Limit (°)	90	80	10	5.2
Extension Stiffness (N·cm/rad)	80	63	17	8.4
Flexion Stiffness (N·cm/rad)	115	77	38	13.3
Rest Position (°)	36	22	14	19.3

Effect of Electrical Stimulation on Passive Properties

The effect of neuroprosthesis (NP) use on the passive properties of the finger joints would be valuable information. Some longitudinal studies designed to answer this question have been started. The passive moment at the second MP joint of one subject, JL, was measured one month following the surgery in which his neuroprosthesis was implanted. Two months later his passive moment was measured again. Figure 1.a.ii.2 shows the remarkable increase in his extension limit and decrease in his extension stiffness that took place within that two month period. The flexion side of JL's MAC was not measured one month after the surgery so as not to strain a tendon transfer of the flexor digitorum superficialis tendon of the long finger to the extensor digitorum communis.

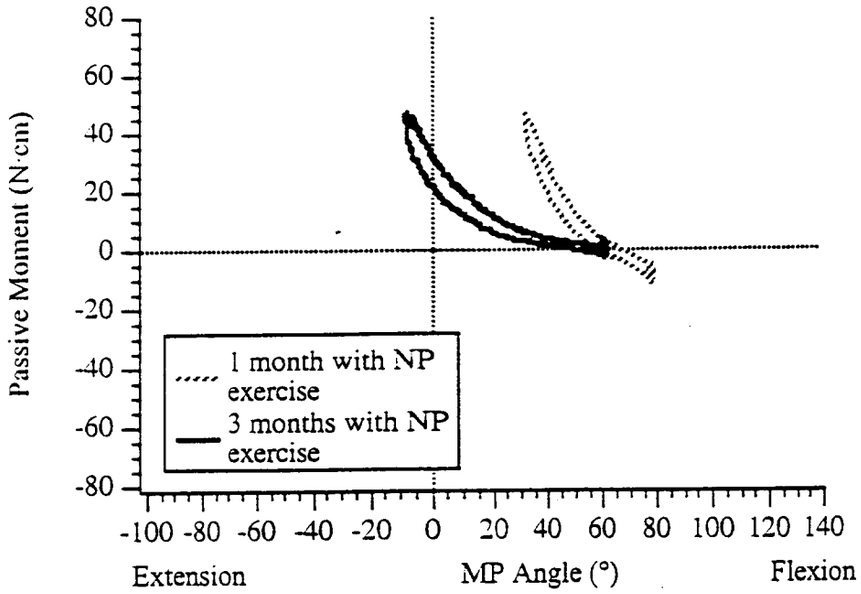

Figure 1.a.ii.2. Extension moment of subject JL showing remarkable improvement in the extension limit and extension stiffness of the index MP joint after a period of two months of exercise with an implanted muscle stimulator.

The only treatment given to JL during the two month post-surgery period was exercise of his intrinsic and extrinsic muscles using electrical stimulation. This suggests that electrical stimulation could improve the passive range of motion and stiffness of a joint.

Diagnosing the Source of Passive Property Disorders

The MAC characterization and the separation of the passive moment into intrinsic and extrinsic components give clues as to both the source of abnormal passive moments and the reason they may be occurring. An example of how the MAC parameters and separation method can be used to locate the abnormal tissues and to suggest their disorder is presented in the following paragraphs.

Subject JL is a 24 year old male with C5 level tetraplegia. He usually wears a splint to keep his left wrist slightly extended. His finger joints rest in a flexed posture and are tight. At the time of his passive moment measurements he had had his NP for three months and it was 4 years and 10 months since his injury. His passive moment measurement results are compared to the average data collected from eight able bodied people in the following three figures .

As Figure 1.a.ii.3a shows, the differences between JL's range of motion parameters and the averages of the able bodied subjects are pronounced. JL's flexion limit is much greater than average, his rest position is much more flexed, and his extension limit is much less than average at all wrist positions. Also, the changes in JL's flexion and extension limits per change in wrist position are greater than those changes shown by the averages of the parameters of the able bodied population.

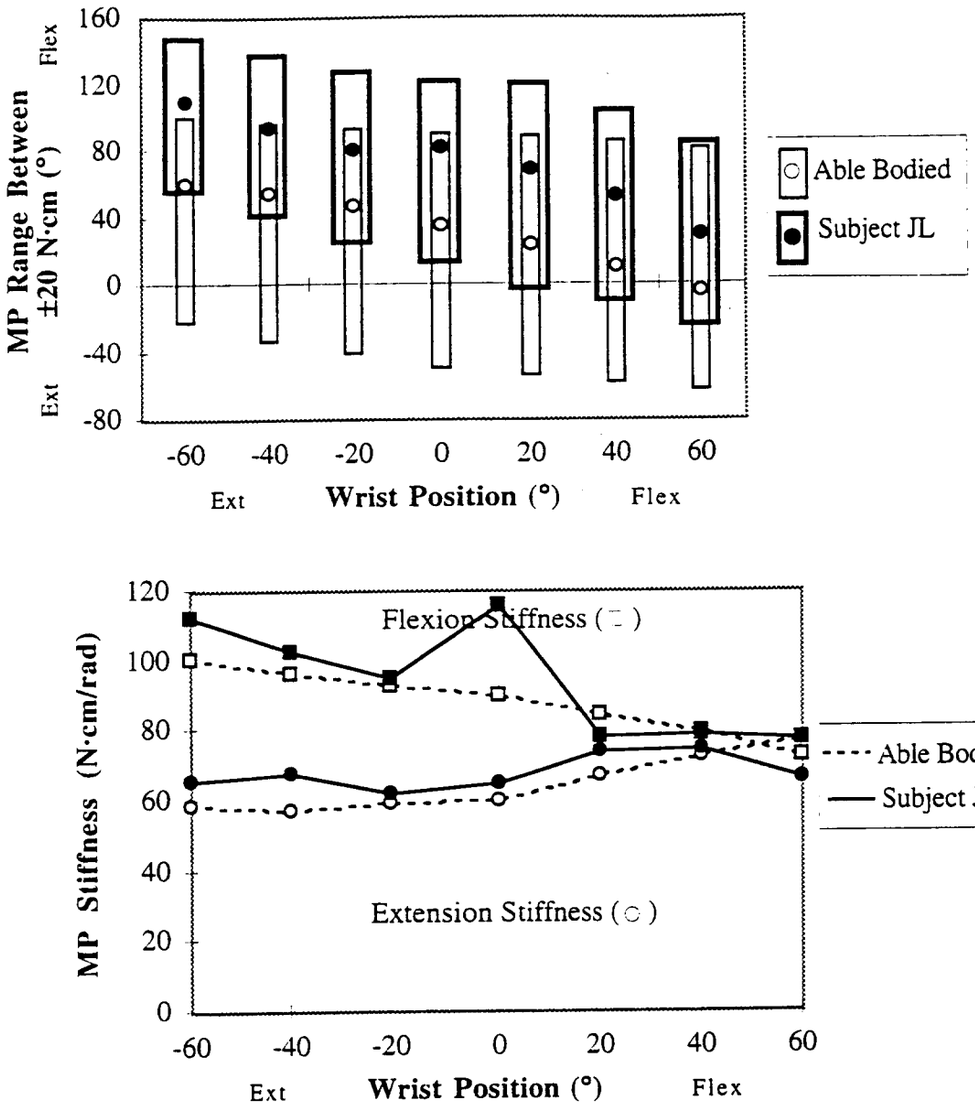

(a)

(b)

Figure 1.a.ii.3. JL's passive moment parameters compared to the able bodied averages. (a) Range of motion parameters. (b) Stiffness parameters.

Although JL's extension limit is less than average at *all* wrist positions, his flexion limit is greater than average at all wrist positions *except* when the wrist is flexed. The greater extension limit would occur if JL's flexor muscles are shorter than average. This would cause his extension limit to be less at *all* wrist positions. Likewise, a longer than average extensor muscle would cause JL's flexion limit to be greater than average at *all* wrist positions. However, as previously stated, JL's flexion limit is not greater than average when his wrist is flexed 60°. There must be an alternative explanation for the increased flexion limits at some, but not all wrist positions.

The fact that JL's flexion limit changed more per wrist position than average suggests that the slack angle of JL's extensor muscles are more wrist dependent than average. This could occur if JL's extensor

muscles were tighter than normal. This doesn't mean his extensors are necessarily shorter, longer, or stiffer than normal, but they are tighter than average so that equal amounts of wrist motion cause a greater than average shift in the passive moment created by JL's extensor muscles. The amount of extensor shift is reflected in the model parameter that correponds to the dependence of the extensor slack angle on wrist position. For JL, this parameter was -0.65, meaning that for every 1° change in wrist position, the slack angle of the extensor muscles (and the passive moment produced by them) shifts 0.65° on the MP joint angle axis. By comparison, the median extensor dependency on wrist position for the able bodied subjects was only -0.28. JL's greater extensor shift is also shown by how JL's percent extensor muscle contribution changes more per wrist position than the able bodied median as shown in Figure 1.a.ii.4b.

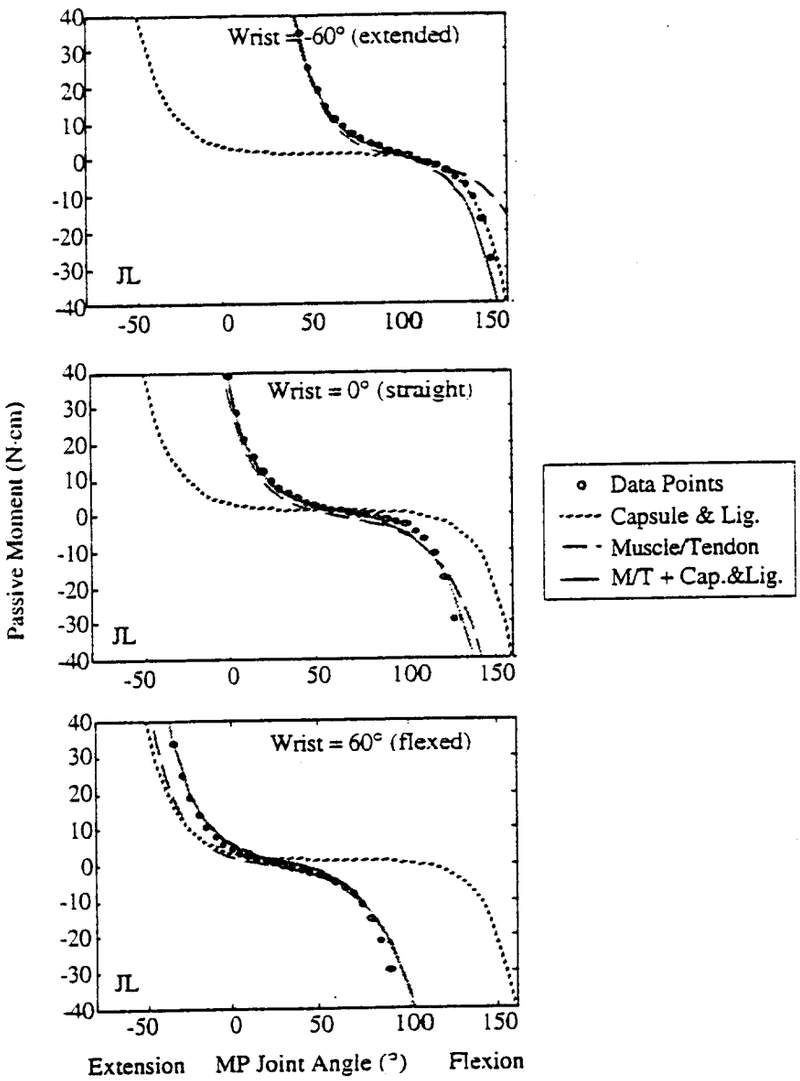

Figure 1.a.ii.4. Results of the separation of JL's total passive moment into intrinsic and extrinsic components.

The nearly linear change in JL's extension limit and flexion limit rules out the possibility of flexor and extensor tendon adhesions. If the change in limits was *perfectly* linear, that would suggest that the passive moment at those limits is produced solely by the extrinsic muscles (assuming a perfectly linear relationship

between the slack length of the muscle/tendon units and the wrist position). Figures 1.a.ii.4 and 1.a.ii.5 show that JL's extrinsic muscles were indeed dominant in producing the total passive moment at the flexion and extension limits. This was especially true of the flexor muscles which were dominant at almost all wrist positions. However, because JL's extension and flexion stiffnesses are not constant in Figure 1.a.ii.3b, it is certain that the proportion of muscles and joint capsular tissues contributing to the total passive moment is changing, as verified by Figures 1.a.ii.4 and 1.a.ii.5.

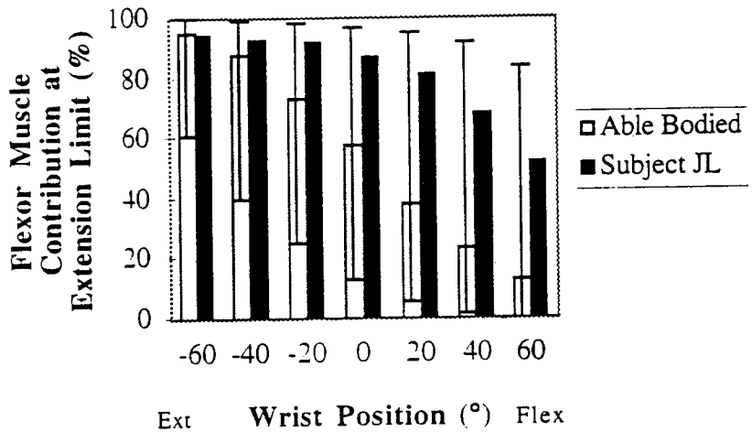

(a)

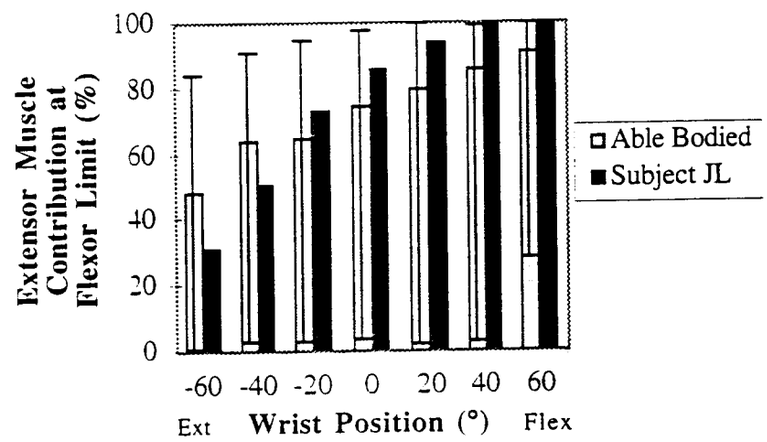

(b)

Figure 1.a.ii.5. JL's percent tendon contribution to the total passive moment compared to the medians of the able bodied population at (a) the extension limit, and at (b) the flexion limit.

Besides the restraining effect of the extensor muscle being diminished more quickly than average as the wrist is extended (greater wrist dependency than average), another cause for JL's greater flexion limit would be a stretched out dorsal joint capsule. This would especially allow greater MP flexion when the wrist is extended. How long or stretched out the dorsal capsule is is reflected in its slack angle, which was another parameter calculated by the model. The slack angle of JL's dorsal intrinsic tissues was 114° while the median was only 79°. This supports the hypothesis that JL's dorsal intrinsic tissues are longer than average. The model also suggests that JL's volar intrinsic tissues are shorter than average. The slack angle of JL's volar intrinsic tissues was 18° while the median was -19°. A shorter volar joint capsule would especially affect JL's extension limit when his wrist is flexed.

This analysis has shown how the model accounts for the differences in the MAC parameters existing between JL and the average data of the able bodied subjects. The results suggest that JL's flexor muscles are shorter than average. An estimate of how much shorter JL's flexors are can be made by multiplying the difference in the extension limit when the wrist is extended by the moment arm of the flexor. The difference in extension limit when the wrist was extended 60° was 77°. Multiplying this by an estimate of 0.8 cm for the flexor's moment arm gives a deficit in flexor length of 1.1 cm. The results also suggested that JL's volar capsule and ligaments are shorter than average, his dorsal capsule is more stretched out, and his extensor muscles are tighter than average. Shortened flexor muscles and volar tissues surrounding the joint capsule and a stretched out dorsal capsule could have been induced by immobilization in a flexed posture. JL's hands have been immobile in flexion for almost five years.

Plans for Next Quarter
The model that separates the total passive moment into intrinsic and extrinsic components will be improved so that the primary data is simulated by the model rather than a curve that is fit to the primary data.

1. b. BIOMECHANICAL MODELING: ANALYSIS AND IMPROVEMENT OF GRASP OUTPUT

Objective
The purpose of this project is to use the biomechanical model and the parameters measured for individual neuroprosthesis users to analyze and refine their neuroprosthetic grasp patterns.

Report of Progress
This project does not start until year three of the project, as described in the proposal. The results from both the magnetic resonance imaging project and the passive moment project will be combined in the biomechanical model to accomplish the goal of improving grasp output. During this quarter we begin making MRI measurements of one individual who had also been characterized using the passive moment measurements.

Plans for Next Quarter
During the next quarter, we continue making MRI and passive moment measurements on the same individuals. This will allow us to incorporate the tendon moment arms into the parameter estimation model for the passive forces. We anticipate that this will allow us to further separate the contributing components of the total passive moment.

2. CONTROL OF UPPER EXTREMITY FUNCTION

Our goal in the five projects in this section is to either assess the utility of or test the feasibility of enhancements to the control strategies and algorithms used presently in the CWRU hand neuroprosthesis. Specifically, we will: (1) determine whether a portable system providing sensory feedback and closed-loop control, albeit with awkward sensors, is viable and beneficial outside of the laboratory, (2) determine whether sensory feedback of grasp force or finger span benefits performance in the presence of natural visual cues, (of particular interest will be the ability of subjects to control their grasp output in the presence of trial-to-trial variations normally associated with grasping objects, and in the presence of longer-term variations such as fatigue), (3) demonstrate the viability and utility of improved command-control algorithms designed to take advantage of forthcoming availability of afferent, cortical or electromyographic signals, (4) demonstrate the feasibility of bimanual neuroprostheses, and (5) integrate the control of wrist position with hand grasp.

2. a. HOME EVALUATION OF CLOSED-LOOP CONTROL AND SENSORY FEEDBACK

Abstract
The purpose of this project is to deploy an existing portable hand grasp neuroprosthesis capable of providing closed-loop control and sensory feedback outside of the laboratory. In this quarter, the portable system configured for grasp force sensory feedback was tested in the hospital for three days with a neuroprosthesis user. The acquire-and-hold test was applied with and without grasp force sensory feedback, but the performance differences were inconclusive.

Purpose
The purpose of this project is to deploy an existing portable hand grasp neuroprosthesis capable of providing closed-loop control and sensory feedback outside of the laboratory. The device is an augmented version of the CWRU hand neuroprosthesis, and was developed and fabricated in the previous contract period. The device utilizes joint angle and force sensors mounted on a glove to provide sensory information, and requires daily support from a field engineer to don and tune. The portable feedback system is not intended as a long term clinical device. Our goal, rather, is to evaluate whether the additional functions provided by this system benefit hand grasp outside of the laboratory, albeit with poor cosmesis and high demands for field support.

Report of Progress
As proposed last quarter, the portable closed-loop system (PCLS) was tested on subject *L* (subject #2, §2.a. QPR4) in the hospital over a three day period. The purpose of these tests was, primarily, to determine whether the acquire-and-hold task could be applied successfully over a complete series of trials with a neuroprosthesis user. Because of other clinical commitments at the time of the hospital stay, *L* was not able to use the PCLS (again configured for grasp force sensory feedback only) outside of the laboratory for significant periods of time. Therefore, the results of the evaluations are not representative of the expected benefits of prolonged exposure to and use of sensory feedback. Rather, the results confirm that the acquire-and-hold task is an appropriate assessment tool.

No significant testing was completed on the first day of the evaluation period due to problems with L's shoulder controller settings and an error in the stimulus frequencies chosen for L's command-level feedback. (The latter is a feature of the NPS IV neuroprosthesis, and consists of an ascending 5-frequency code representing increasing command levels in 20% steps, delivered through an implanted electrode in a sensate area.) A combination of posture, shoulder weakness, small range of shoulder motion, and marginal placement of the shoulder angle transducer yielded frequent inadvertent locks, and difficulty in unlocking. *L* was subsequently given a wrist controller with switch lock for the balance of the day. The stimulus frequency (16 Hz) assigned to the 80-100% command range was too high and produced uncomfortable sensations. This same frequency, however, had been set for ~1.5 years without reports of discomfort. It only became apparent after the command range was spanned fully either by manual elevation of the shoulder controller by an investigator, or by computer-controlled changes in command level. It is possible that this subject never exceeded 80% command in daily use (see below). The maximum frequency was lowered slightly (14 Hz) to alleviate the discomfort.

Preliminary tests were completed on the second day using the shoulder controller and with locks disabled. As in prior tests with this user, the range of stimulus currents for the grasp force feedback was quite narrow (2.94 - 6.10 mA). The user reported being able to feel a gradation in perceived stimulus amplitude, increasing with force. However, the user's verbal responses were ambiguous, and it is not clear that the user differentiated the intensive code used for force feedback from the more familiar frequency code used for command feedback. The user also reported that the perceived amplitude did not change appreciably over the first half of the stimulus range. If uncertainties persist with other subjects, it may be necessary to use bite force - stimulus current matching to orient the user, as proposed in an earlier project (NS-9-2355).

The currents were mapped to an output force range of 0.50 - 4.57 N using a log-log transformation as described previously.

Representative results from the trials are shown in Fig. 2.a.1. The uppermost plot (A) shows one of the practice trials, with knowledge of results *KR* (user viewed trajectories after trial was complete), with vision *V* (user viewed trajectories in real time during the trial), but without sensory feedback *FB*. In all trials, the total duration was 5 sec, with a 3-sec acquire phase and a 2-sec hold phase. These times were chosen to accommodate the user's coordination and speed limitations. The target window was set to 80±20% command. In this particular case, that setting resulted in a force window between 1.78 and 3.65N (horizontal dashed lines). The trajectories show that the user had difficulty reaching intermediate forces since small changes in command between roughly 60-80% produced large changes in force. Fig. 2.a.1.(B) shows two trials, each from a set of 16 replicate trials; the first without sensory feedback and the second with sensory feedback. Feedback had little effect on the overall success rates (1/16 and 3/16, respectively) but anecdotal observations suggest that the feedback helped the user make small changes in command and find the intermediate level required by the target window.

Similar trials were completed on the third day. In this case, however, the success rates changed markedly: 8/16 vs 15/16, without and with *FB* respectively. This difference is deceptive, though, because the subject was able to keep the force in the target window by simply exerting the maximum command (see Fig. 2.a.1.(C)) due to a slight mismapping between command and maximum force. (Also, the target window was set erroneously to include 100% command.) However, the user only learned how to achieve that command with the sensory stimulation. Afterward, the user was able to complete the task successfully with or without sensory feedback. If the user's posture or zero point had changed, it is likely that the task would have to be re-learned in the absence of force feedback.

The results overall are inconclusive, due in part to a poor choice of target window and the absence of long exposure to the feedback. Further examination of the data does suggest particular control problems that may be mitigated by force feedback. The trajectories in Fig. 2.a.1 show that the command-to-force relation is highly nonlinear and the force output is delayed significantly relative to the command input. Both characteristics were estimated from one data set (16 trials without FB, day 2) as follows. The recruitment nonlinearity was calculated from the hold phases of all trials in the set in which the coefficient of variation of the force and command were less than 15% (i.e., command did not change significantly so the system dynamics are irrelevant). The force F is plotted as a function of command C in Fig. 2.a.2, and is fit with a Weibull function of the form:

$$F = K\left[1 - e^{-(C/\beta)^{\alpha}}\right] + B$$

Note that the recruitment function agrees with the observation made earlier that the output changes little over most of the command range, and rises sharply between 60-80% command. In other words, this user has only 20% of the available command range to control force. The complete force trajectories were then fit assuming that the command was converted to force using the Weibull fit, and then delayed an amount ∂T = 400 msec, which produced the best agreement. The results are shown in Fig. 2.a.3, where the solid lines are the actual forces and the dashed lines are the predicted forces. The forces are predicted quite well apart from the apparent low-pass characteristic of the real system. (Note that the delay as calculated includes both a pure delay plus the delay that would be produced by the low-pass characteristic of the activation-contraction coupling.) In other words, user L had to accommodate two significant control problems: a static nonlinearity and a 400 msec delay. Sensory feedback could help with the former but not the latter. That is, L could attend to the sensory feedback and attempt to produce some intermediate, criterion value — but that feedback would still lag the shoulder position by 400 msec.

Plans for Next Quarter
User *L* was asked to participate in the full 9-week evaluation protocol, and expressed initial interest pending discussions with family and caregivers. If *L* agrees, we will initiate the complete protocol. *L* has been equipped with wrist control, however, which obviates use of closed-loop control, but still permits evaluation of sensory feedback.

2. b. INNOVATIVE METHODS OF CONTROL AND SENSORY FEEDBACK

2. b. i. ASSESSMENT OF SENSORY FEEDBACK IN THE PRESENCE OF VISION

Abstract
The purpose of this project is to develop a method for including realistic visual information while presenting other feedback information simultaneously, and to assess the impact of feedback on grasp performance in the presence of such visual information. In this quarter, the video acquisition system was used to collect an initial set of video clips.

Purpose
The purpose of this project is to develop a method for including realistic visual information while presenting other feedback information simultaneously, and to assess the impact of feedback on grasp performance. Vision may supply enough sensory information to obviate the need for supplemental proprioceptive information via electrocutaneous stimulation. Therefore, it is essential to quantify the relative contributions of both sources of information.

Report of Progress
The video simulation system has 3 major components: (1) a recording system used to create the video clips and accompanying command, force and span data files; (2) a playback system that permits those files to be displayed according to the command signal generated by a test subject; and (3) an evaluation system that implements an acquire and hold task, as in the PCLS study. In this quarter, the recording system was used successfully to record an initial set of video clips from two neuroprosthesis users (one was user *L* discussed above).

An initial plan for implementing the evaluation software has also been formulated. For evaluation of sensory feedback, the software programmed for the PCLS evaluation can be used directly. That is, the PCLS will be used to measure the command signal, which can be made available for external processing via an additional breakout connector. The command can then be recorded by the video playback software, resulting in display of the appropriate video frame and output of a voltage corresponding to the expected output of the force sensor. The latter signal is substituted for the actual sensor signal normally measured by the PCLS host computer running the evaluation software. The only disadvantage to this configuration is that it requires both the PCLS and the host computer, and cannot be run simultaneously with at-home evaluations of the portable system.

Plans for Next Quarter
The video clips collected this quarter will be processed and used in conjunction with the evaluation software for initial testing of the complete simulation system with able-bodied subjects.

2. b. ii. INNOVATIVE METHODS OF COMMAND CONTROL

Abstract
During this quarter we focused on analysis of the performance of a 2-element strain gage mounted on the thumbnail as a force sensor and a contact sensor. A model of the grasp force as a linear function the output of the two strain gages was highly correlated with the actual grasp force and was able to predict the

grasp force with a low rms error. Optimization of filter order, cut-off frequency, and amplitude thresholds indicated that the gages could be used to detect contact, without detection of false positives, but that the optimal parameters varied across objects.

Purpose

The purpose of this project is to improve the function of the upper extremity hand grasp neuroprosthesis by improving user command control. We are specifically interested in designing algorithms that can take advantage of promising developments in (and forthcoming availability of) alternative command signal sources such as EMG, and afferent and cortical recordings. The specific objectives are to identify and evaluate alternative sources of logical command control signals, to develop new hand grasp command control algorithms, to evaluate the performance of new command control sources and algorithms with a computer-based video simulator, and to evaluate neuroprosthesis user performance with the most promising hand grasp controllers and command control sources.

Report of Progress

During this quarter we focused on analysis of thumbnail-mounted strain gages as contact and grasp force detectors. As described previously (QPR#4), the output of a metal foil strain gage rosette glued to the thumbnail using cyanoacrylate cement was recorded during grasp, transport and release of a variety of standardized objects. In addition to the standard cylinders and blocks (see QPR#2), trials were also conducted with an instrumented "book" [Memberg and Crago, 1997] which provided a voltage output proportional to the grasp force. Each trial consisted of the subject reaching out, grasping, lifting the object, transporting it to another location 30 cm above the first, and releasing the object. The object was then re-grasped, lifted, and returned to the starting point. Each of 4 subjects completed 4-6 trials with each object and used both lateral and palmar grasp.

USE OF STRAIN GAGE SIGNALS TO DETERMINE GRASP FORCE

The purpose of this analysis was to determine whether the strain signals could be used as grasp force sensors.

Methods

The output of the two gages, one oriented longitudinal to the thumbnail (L) and one oriented transverse (T) to the thumbnail, were used to predict grasp force using a number of different models. The grasp force predicted by the models was compared to the actual grasp force as measured by the instrumented book.

In the first two models, the force was a linear function of the output of one or the other gage:

$Force=m*L+b$ (1) $Force=m*T+b$ (2)

In the second two models, a second order term was included

$Force=m_1*L+m_2*L^2+b$ (3) $Force=m_1*T+m_2*T^2+b$ (4)

The third model used the sum of the output of both gages to predict the force

$Force=m*(L+T)+b$ (5)

The fourth model used the output of both gages individually to predict the force

$Force=m_1*L+m_2*T+b$ (6).

The model parameters in each case were determined by least squares regression with data from one trial of palmar grasp, one trial of lateral grasp, or a concatenated set of one palmar and one lateral grasp trial. The ability of each model to predict the contact force in the trial from which the parameters were determined was evaluated using the regression coefficient (r^2).

Once the best among these model was identified (#6) we determined the ability of the model to predict force under conditions other than those used to identify the model parameters. Average model parameters were estimated from data across all palmar trials or all lateral trials within a subject. The root mean square (rms) error between the actual force on a given trial and the force predicted with the average parameters

was compared to the rms error between the actual force on a given trial and the force predicted with the parameters obtained with the data from that trial.

Results

The results of the analysis of the six force models is shown in Figure 2.b.ii.1. Each panel shows the individual and mean regression coefficients obtained with each of the six models when fitting 22 trials of palmar grasp (fig. 2.b.ii.1A), 22 trials of lateral grasp (fig. 2.b.ii.1B), or 21 trials of concatenated palmar and lateral grasp data (fig. 2.b.ii.1C) from 4 subjects. The mean regression coefficients across all data are presented for each model in Table 2.b.ii.1.

Table 2.b.ii.1: Mean regression coefficients for six different force models.

Data/Model	mL+b	mT+b	$m_1L+m_2L^2+b$	$m_1T+m_2T^2+b$	m(L+T)+b	m_1L+m_2T+b
Palmar	0.30	0.77	0.37	0.81	0.50	0.80
Lateral	0.54	0.90	0.58	0.91	0.79	0.94
Pal+Lat	0.25	0.77	0.39	0.82	0.50	0.83

The results of models 1 and 2, where the force was a linear function of the output of either the longitudinal or transverse gage indicated that the transverse gage gave a better prediction of the force than did the longitudinal gage across data sets. When the models were extended to include second order terms of the individual gage outputs (models 3 and 4) the force prediction improved for both gages, and across all data, although the improvements were smaller for the transverse gage than the longitudinal gage. Including data from both gages with a single gain parameter (model 5) improved force prediction over the longitudinal gage only models, but was worse than the transverse gage only models. The best force prediction was achieved by including data from both gages with individual gain parameters (model 6). This model gave improved performance over the all models and across all data sets, except model 4 with palmar data, where the performance was equivocal.

Model 6 was used to determine the ability of the gage outputs to predict grasp force using regression parameters obtained under conditions other than those under test. Model parameters were obtained four different ways: from fitting data on a given trial (trial to trial) or using the within subject average parameters across trials (average across palmar trials, average across lateral trials, or average across concatenated trials of both lateral and palmar data). The results of this analysis are shown in Figure 2.b.ii.2. Each panel shows the root mean square (rms) error between the actual force in a trial and the force predicted using model 6 and the output of the two gages for 22 trials of palmar grasp (A) and 22 trials of lateral grasp (B) across four subjects. The average rms errors across all data are presented for each parameter set and the different data sets in Table 2.b.ii.2. It is important to note that the five highest rms errors, which appear as outliers, were all from the same subject. When the strain gage was removed from this subject it was apparent that it was bonded to the nail over only ~50% of its area.

The smallest rms errors were obtained when using parameters fit from data of a given trial to predict the force for the same trial. The largest rms errors were obtained when using the average parameters from lateral grasp trials to predict the force in palmar and lateral trials. Importantly, the average parameters from the concatenated data trials were able to predict both palmar and lateral data with rms errors only twice as large as those obtained using trial to trial parameter fits.

Table 2.b.ii.2: Average rms errors predicting force during palmar grasp and lateral grasp with different sets of model 6 parameters.

Model Parameters	palmar data	lateral data
trial to trial	0.280	0.384
average palmar	0.332	1.82
average lateral	6.27	2.26
average palmar+lateral	0.508	0.622

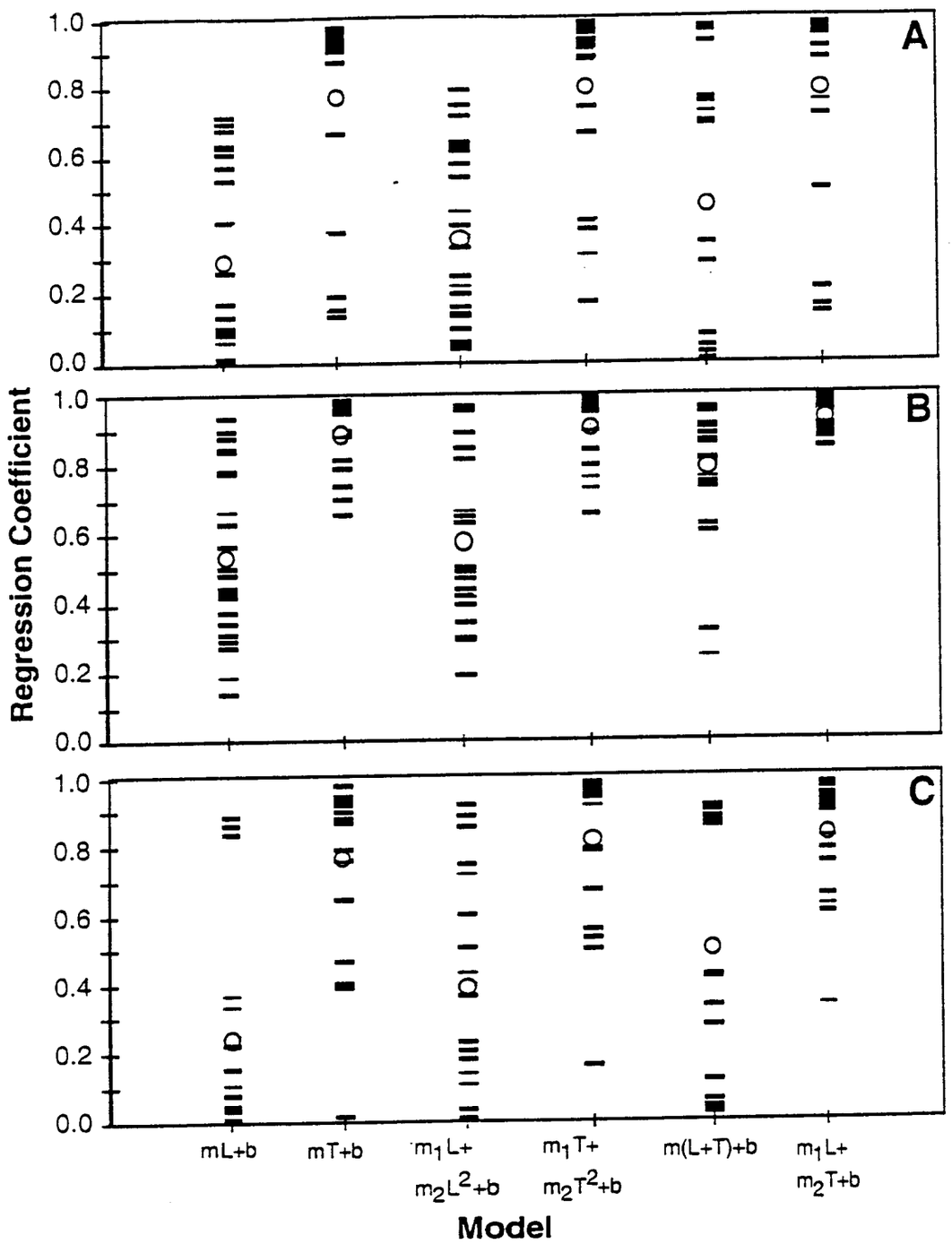

Figure 2.b.ii.1: Individual (horizontal bars) and mean (open circles) regression coefficients obtained with each of the six force models when fitting 22 trials of palmar grasp (A), 22 trials of lateral grasp (B), or 21 trials of concatenated palmar and lateral grasp data (C) from 4 subjects.

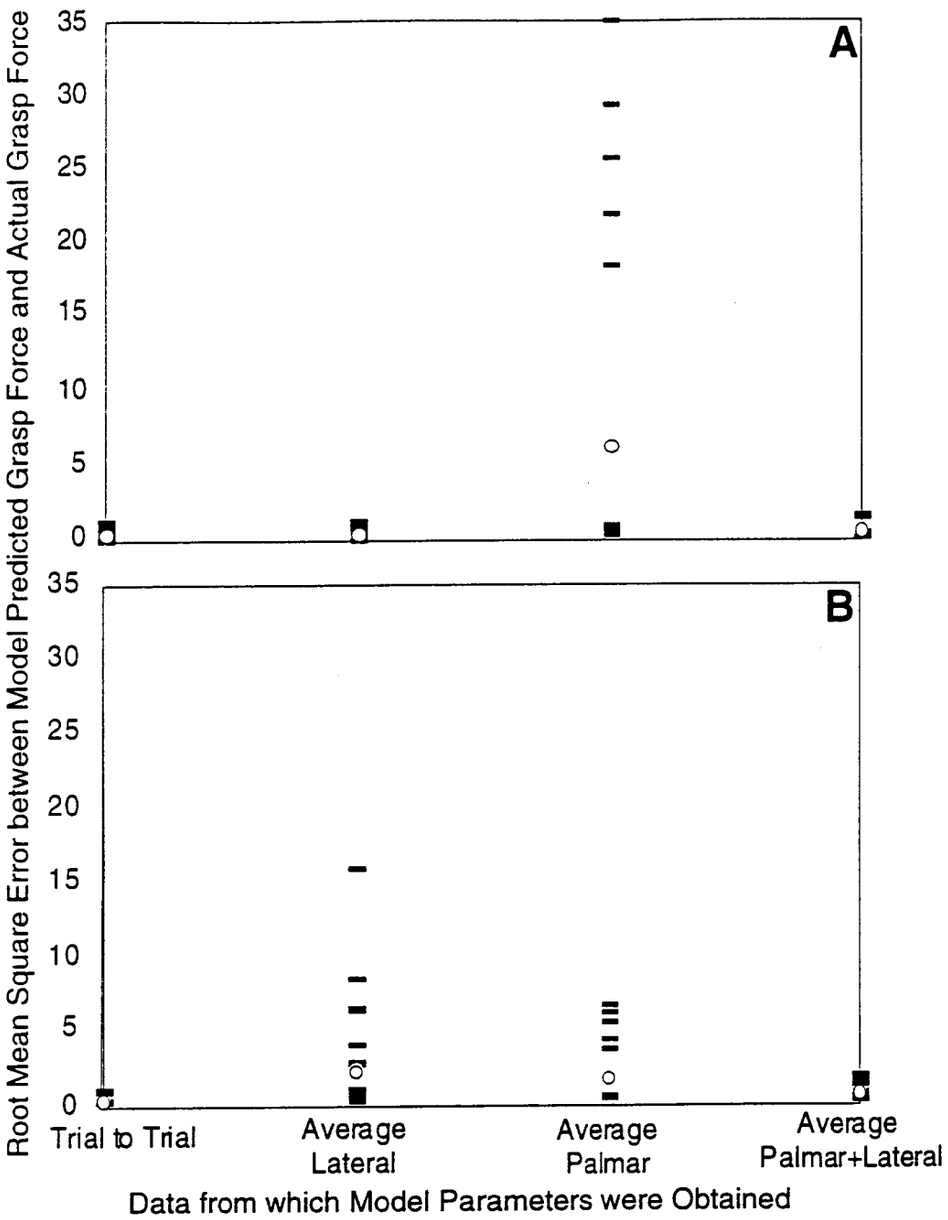

Figure 2.b.ii.2: Individual (horizontal bars) and mean (open circles) root mean square errors between the actual force and the force predicted using model 6 with different sets of parameters for palmar (A) and lateral (B) grasp trials.

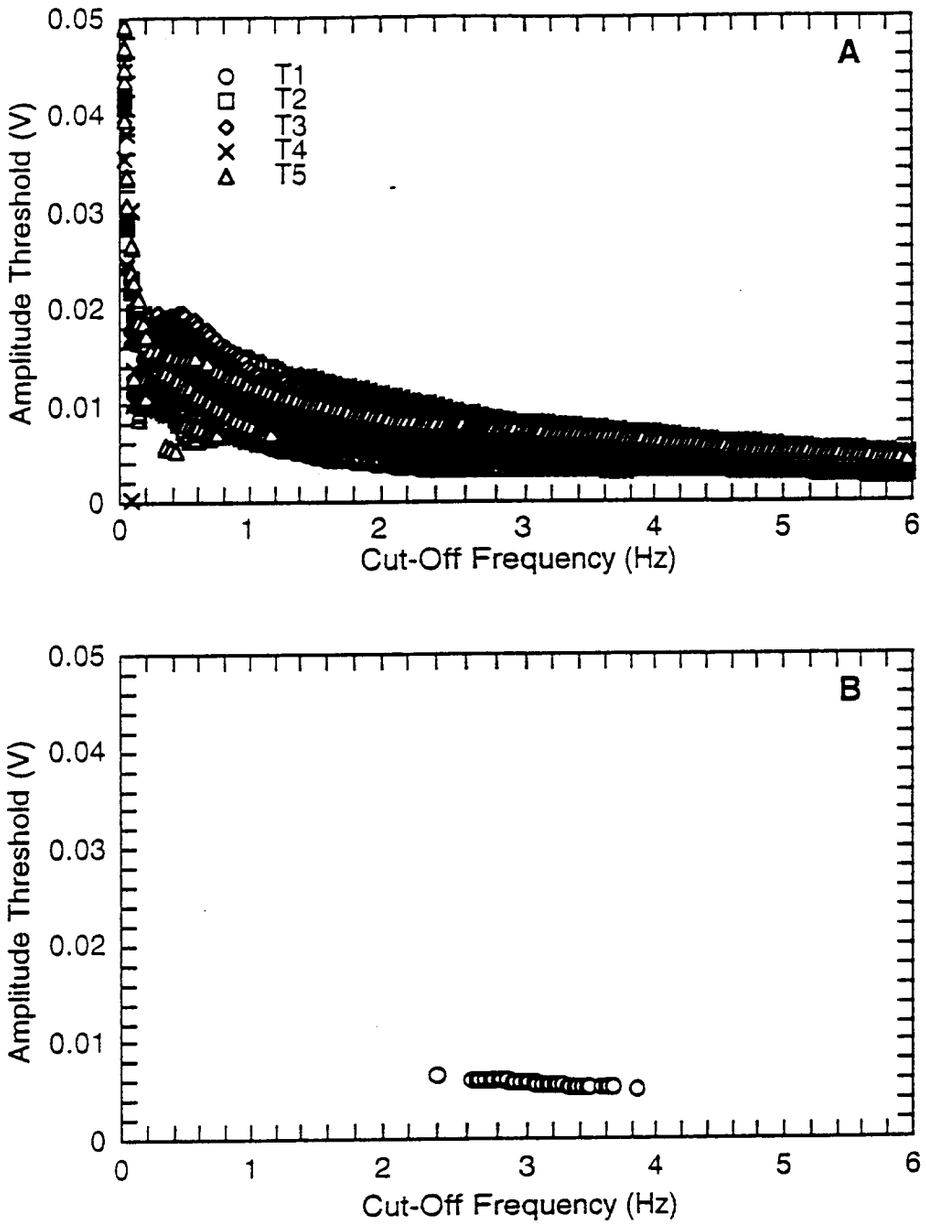

Figure 2.b.ii.3: (A) Combinations of cut-off frequency and threshold value which met the performance criteria of true positives=4 and false positives=0 (i.e., ideal performance) in each of five trials. The different symbol types represent five different trials with 1 object (Block 2) in lateral grasp with 1 subject. (B) Combinations of cut-off frequency and threshold value which met the performance criteria of true positives=4 and false positives=0 in all five trials.

USE OF STRAIN GAGE SIGNALS TO DETERMINE OBJECT CONTACT

As described in previous progress reports we have been examining nail mounted strain gages as grasp contact detectors. During this quarter we focused on optimizing the signal processing algorithm to maximize the detection of true positives (detection of contact when contact is present) and minimize the detection of false positives (detection of contact when contact is not present). We used a "brute-force" approach to try all combinations of cut-off frequency and threshold and set performance criteria to determine which combinations gave the best performance.

Methods

Initial analysis with the signals from the lateral and transverse gages indicated that the sum of the two signals provided the highest signal to noise ratio. The summated signal was filtered with a first or second order Butterworth high pass filter to eliminate drift and to isolate changes in output that occur during contact. An amplitude threshold detector with hysteresis was then used to detect contact from the summated signal. The number of true positives and number of false positives was quantified while varying the cut-off frequency of the filter and the amplitude of the threshold detector.

A positive contact signal was generated independently with an electronic circuit (see QPR #2). A true-positive was registered if the gage generated contact signal corresponded to the positive contact signal within a small (167 ms) window. Note that timing of positive contact signal was delayed by an amount appropriate for the filter, and that these delays would be present in a real-time application of this technique.

Table 2.b.ii.3: Number of combinations of cut-off frequency and threshold value which met the performance criteria in each of five trials (TP=true positives, FP=false positives) for first- (1^o) and second-order (1^o) highpass filters with object "Block 2". "Common" indicates the number of combinations of cut-off frequency and threshold value which met the performance criteria in all five trials.

Trial	1^o, TP≥3, FP=0	1^o, TP=4, FP=0	1^o, TP=4, FP≤1	2^o, TP≥3, FP=0	2^o, TP=4, FP=0	2^o, TP=4, FP≤1
1	3063	1528	1580	1799	521	595
2	5223	2438	2714	1417	676	861
3	4786	1699	1716	2370	552	659
4	6906	2525	2531	1631	482	683
5	5263	2024	2076	2175	453	591
Common	1453	37	41	14	0	0

Results

The combinations of cut-off frequency and threshold which produced the desired performance criteria varied with the rigor of the criteria, the order of the filter, the object being grasped, and across trials. The entries in Table 2.b.ii.3 are the number of combinations of cut-off frequency and threshold value which met the performance criteria in each of five trials, as well as the number of combinations of cut-off frequency and threshold value which met the performance criteria in all five trials (i.e., combinations common to all trials). The condition of 4 true positives and 0 false positives (TP=4, FP=0) represents ideal performance. For this object and this subject there were 37 combinations of cut-off frequency and threshold value which yielded ideal performance in all trails when a first-order filter was used, but no combinations that yielded ideal performance across all trials when a second-order filter was used. If the performance criteria were relaxed to allow one contact to be missed (TP≥3) or to allow 1 false positive (FP≤1) then the number of combinations of cut-off frequency and threshold value which met the criteria increased for each trail, and increased when considering points common to all trials.

Figure 2.b.ii.3A shows the combinations of cut-off frequency and threshold value which generated ideal performance (true positives=4, false positives=0) in each of the five trials with the object, "Block 2" in lateral grasp with 1 subject. It is clear that the ideal combinations spanned a limited region of parameter space and that there appeared to be areas common to different trials. Figure 2.b.ii.3B shows the 37

combinations of cut-off frequency and threshold value which met the performance criteria of true positives=4 and false positives=0 in all five trials.

These results indicate that the performance of nail mounted strain gages as contact detectors can be ideal if the right combinations of filter cut-off frequency and amplitude threshold are selected. This approach yielded a significant improvement in performance over that found when using cut-off frequencies and thresholds selected by eye (see QPR#2). However, the approach of searching the entire parameter set and determining performance at each point required approximately 24 hours of computer time for five trials! Thus, in the next quarter we will continue this analysis using constrained optimization techniques to identify the optimal processing parameters.

Plans for Next Quarter

The results obtained in this quarter indicate that the nail mounted strain gages can function as both grasp force sensors and contact detectors, but that performance is sensitive to the force model selected and to the parameters used to detect contact.

During the next quarter we will continue analysis of strain signals for force sensing and contact detection. We will use a non-parametric identification technique to find the optimum linear model to predict grasp force. We will use constrained optimization to identify the optimal parameters for contact detection without having to search the entire parameter space. We will also conduct a review of commercially available accelerometers to identify the best accelerometer to mount on the thumb as a slip detector during grasp.

References

Memberg, W.D., Crago, P.E. (1997) Instrumented objects for quantitative evaluation of hand grasp. Journal of Rehabilitation Research and Development 34(1):82-90.

2. b. iii. INCREASING WORKSPACE AND REPERTOIRE WITH BIMANUAL HAND GRASP

Abstract

Alternate control methods were investigated for a possible solution to the command control problem that the bilateral implementation of the neuroprosthesis presents. The current control methodologies (e.g. external transducer, external switch, myoelectric control) have limitations which prevent them from effectively operating the bimanual system. Studies were also continued on evaluating the intrinsic muscles for incorporation into the neuroprosthesis. Moment measurements were made on the extrinsic and intrinsics muscles in two subjects with the 10 channel implant. This data is in the final stages of analysis for future presentation in a scientific publication.

Purpose

The objective of this study is to extend the functional capabilities of the person who has sustained spinal cord injury and has tetraplegia at the C5 and C6 level by providing the ability to grasp and release with both hands. As an important functional complement, we will also provide improved finger extension in one or both hands by implantation and stimulation of the intrinsic finger muscles. Bimanual grasp is expected to provide these individuals with the ability to perform over a greater working volume, to perform more tasks more efficiently than they can with a single neuroprosthesis, and to perform tasks they cannot do at all unimanually.

Report of progress

1. Alternate control methods

In this quarter, an intensive review of the possibility of using cortical signals to operate the neuroprosthesis was conducted. The current neuroprosthesis allows for three possible methods of controlling the system: 1) the use of an external transducer located on the contralateral shoulder or the ipsilateral wrist, 2) the use of external switches or 3) the use of processed myoelectric signals. However, each of these methods have limitations, which is becoming more evident with the bilateral implementation

of the neuroprostheses. For example, the preferred method of controlling the neuroprosthesis is to mount the external transducer on the wrist of the same arm that has received the neuroprosthesis. However, if the subject was injured at the C5 level, they lack active wrist extension. Therefore, the contralateral shoulder must be used as a control site. If a neuroprosthesis has been implanted in that arm as well, as in the case of subject JHJ (QPR #4), a transducer on that shoulder would interfere with the operation of the neuroprosthesis on that side.

The solution to this problem has been to use either external switches or myoelectric signals recorded from the brachioradialis or the platysma muscles. However, from observation of the subject performing activities of daily living (ADL) tasks, it is evident that the external switches are not the ideal method of control. This is clearly the case when the subject is holding an object in one hand, and must then depress the external switches to operate the neuroprosthesis in the other hand. The subject may be unable to depress the switch, require a long period of time to operate the system, or the object may become dislodged from his hand. The use of the myoelectric signals has also presented some difficulties with this subject, particularly with the subject isolating the activation of the brachioradialis to act as a control site and with stimulus artifact corruption of the myoelectric signal.

One possible solution to the control problem is the use of voluntarily controlled cortical activity for a control source. The studies of Wolpaw (Wolpaw, et al, 1991; McFarland, et al, 1997; Wolpaw & McFarland, 1994) have indicated that subject can be trained to voluntarily control the amplitude of the mu rhythm, as recorded by the electroencephalogram (EEG). The mu rhythm is an 8 - 12 Hz frequency signal that is recorded over the central sulcus and is associated with the activation state of the motor cortex. Subjects have been trained to use this signal to operate vertical cursor movement on a computer screen. This control over cursor movement has multiple applications in assistive technology, and as a possible control site for the operation of a neuroprosthesis. These studies differ from Humphrey (Humphrey, et al., 1993; Humphrey, et al., 1970; Humphrey & Tanji, 1991) and Schwartz (Schwartz, 1993; Schwartz, 1994) in that 1) the recording of the brain activity is nonintrusive and 2) subjects are trained to generate a specific signal that can be interpreted, instead of trying to interpret brain activity.

There are several questions which need to be addressed about the EEG signal before the signal can be used to operate a neuroprosthesis. Subjects in these studies were seated comfortably and asked not to move while generating cursor movement. This is because movement of the extremities causes attenuation of the mu rhythm. Although this is not a problem in the target population of this device (individuals with advanced ALS), it presents a problem in operation of a neuroprosthesis where the subject will be talking and making movements of the hand, trunk, elbows and shoulders. Therefore, it must be known if subjects can be trained to compensate for this interference, or if additional signal processing techniques can be applied to acquire a signal. Another question raised in the use of the EEG signal to control the operation of the neuroprosthesis involves the fundamental differences which exist between the motor cortex of an able bodied subject and a person who has sustained tetraplegia. After a spinal cord injury, the motor cortex reorganizes itself so that the remaining voluntary movement is remapped on the cortex. Whether this remapping will allow the neuroprosthesis user to exert greater control over the mu rhythm or if it will be a hindrance have yet to be studied. There are also questions about signal repeatability and the subjects ability to achieve different levels of activation which are also important for the operation of the neuroprosthesis. These questions, as well as the establishment of a control strategy for use with the EEG signal and the overall feasibility of an EEG controller, will be the focus of later studies.

Preliminary work has begun on the development of the cortical controller for the neuroprosthesis. During this quarter, we have begun discussions with Dr. Jonathan Wolpaw and his colleagues at the Wadsworth Center for Labs and Research in Albany, NY on the feasibility of using their technology to operate a neuroprosthesis. This led to a two week visit to the Wadsworth Center, at which time the instrumentation and protocols which have been developed by this group were studied. With the help of Dr. Wolpaw, we have now begun to construct our own EEG-based brain-computer interface (BCI) so that we can start training subjects to operate the system. We can then analyze the data to derive a control strategy which will allow control of the mu rhythm to be converted into operation of the neuroprosthesis. The final step will be to interface the two systems using the derived control strategy. We will then evaluate the feasibility of cortical control and determine system limitations for further refinement.

2. *Muscle Moment Measurements*

Studies were conducted on two neuroprosthesis users who have received the 10 channel implantable stimulator. Table 2.b.iii.1 shows the breakdown of the types of electrodes implanted in each muscle for each subject. In both subjects, a combination of epimysial and intramuscular electrodes were implanted. The first subject had intrinsic electrodes implanted into the second and fourth metacarpal spaces, while the second had the electrodes implanted in the second and third metacarpal spaces.

Methods

The methodology used for both subjects was as follows. The arm of the subject was placed on a platform with the wrist fixed at 0° of extension, the forearm pronated at 90°, and the elbow fixed at 30-45° of flexion, depending on what was comfortable for the subject. The finger moment transducer, which has been described in previous reports, was fixed to the hand. Each of the joints of the fingers were set by the device at 10° of flexion. The neuroprosthesis was then connected to a PC computer to allow for control over the activation of each muscle to be studied. For these subjects, the muscles studies were the extensor digitorum communis (EDC), the flexor digitorum superficialis (FDS), the flexor digitorum profundus (FDP), and the intrinsic electrodes. Moments for each of these muscles were measured at five pulsewidths from 0 μs to the maximum (i = 20 mA, f = 12.5 Hz). The moment at each pulsewidth was recorded five times, averaged from the last 50 samples of a three second sampling period (100 Hz sampling frequency).

	Subject 1	**Subject 2**
Hand	right	left
Electrode used		
Extrinsic Muscles		
FDS	Epi	MIM
FDP	MIM	MIM
EDC	Epi	Epi
PQ		Epi
Triceps	MIM	
EPL	Epi	Epi
FPL	Epi	Epi
Intrinsic Muscles		
AdP	MIM	Epi
AbPB	MIM	Epi
2DI	MIM	MIM
3DI		MIM
4DI	MIM	
Synchronizations	None	None

Epi = Epimysial Electrode
MIM = Memberg intramuscular electrode

Table 2.b.iii.1 - Electrodes used in the two subjects in this study with the 10 channel implantable stimulator.

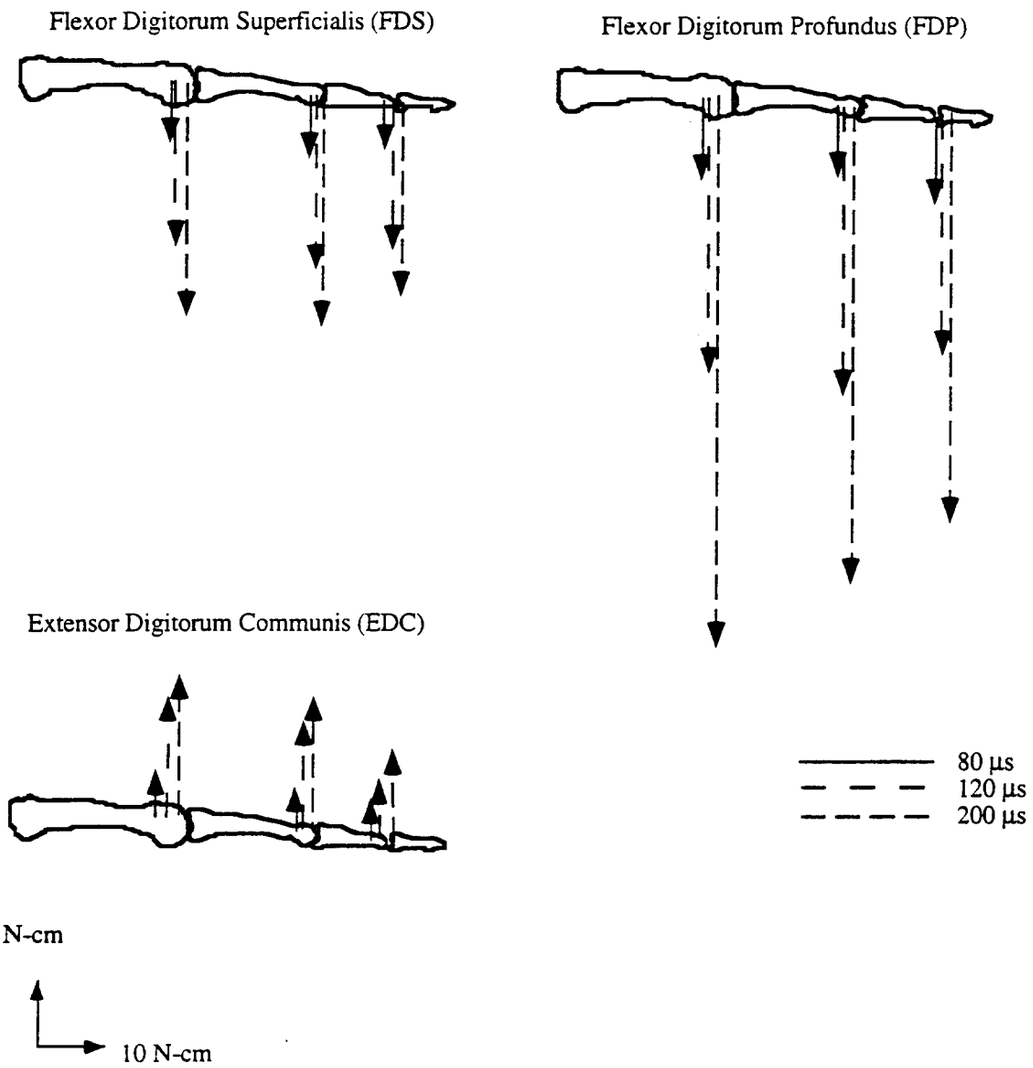

Figure 2.b.iii.1 - Extrinsic Muscle Moments for Subject 1 (Long Finger Only)

Results

The moments measured for the extrinsic muscles in subject 1 are shown in Figure 2.b.iii.1. Only the long finger is shown for clarity of presentation. The vectors pointing up indicate extension while the arrows pointing down indicate flexion. With increasing pulsewidth, the magnitude of the moment also increases, represented by the length of the vector. The actions of the FDP and EDC muscles in this subject are what would be expected, based upon the anatomy of these muscles and the experimental constraints. However, the actions of the FDS muscles, generating a flexion moment at the distal interphalangeal joint, were unexpected. Subject movement and device failure have been ruled out as possible causes for this

discrepancy. Other explanations which have yet to be fully investigated are possible activation of the FDP muscle when the FDS is activated, and tendon adhesions between the FDS and FDP muscles.

The moment measurements made on the intrinsic muscles of both subjects at the metacarpophalangeal (MP) joint are shown in Figure 2.b.iii.2. The view represented in this figure is of one looking down the hand from the fingertips. Only the maximum pulsewidths are shown in this case, again for clarity of presentation. From this data, the following can be concluded. First, the placement of the intrinsic electrodes into the metacarpal spaces, in most cases, led to activation of the other intrinsic muscles (primarily the volar interossei) which provided additional function. The only case where this did not occur was with the 4DI electrode in subject 1. Second, the placement of the electrodes into the second and third metacarpal spaces (subject 2) is a much better placement than electrodes into the second and forth metacarpal spaces (subject 1). The placement of the electrodes in subject 1 led to a pulling apart of the fingers, which is a functionally inadequate grasp. Finally, the electrical stimulation of the dorsal interossei led to small moments in the abduction/adduction direction. This indicates that the electrodes were placed into the volar component of the muscle, which is responsible for flexion at the metacarpophalangeal joint and extension of the interphalangeal joints. This finding corresponds with the surgical implantation of theses muscles, which was as deep in the muscle as possible to get additional activation of the volar interossei muscles located in the same metacarpal space.

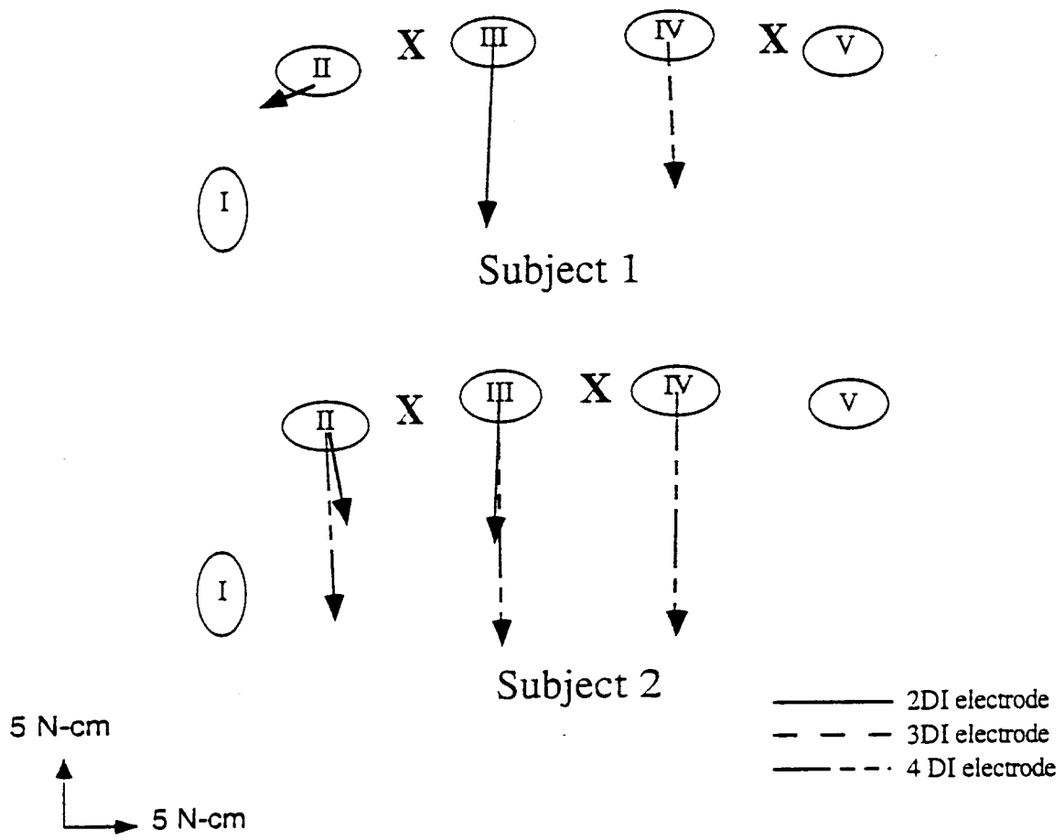

Figure 2.b.iii.2 - Intrinsic Moment "Vectors" at the MP Joint

Plans for Next Quarter
During the next quarter, the analysis of the intrinsic muscle data will be completed, and this study will be submitted to a scientific publication. In addition, more work will be conducted on the possibility of using cortical signals to operate the bilateral system.

References

Humphrey, D., Schmidt, E., & Thompson, W. (1970). Predicting Measures of Motor Performance from Multiple Cortical Spike Trains. Science, 170, 758-762.

Humphrey, D., Reed, D., Mewes, K., & Hochberg, L. (1993). Cortical Control of Neural Prosthetic Devices (Quarterly Report 7): Neural Prosthesis Program, National Institute of Neurological Disorders and Stroke, National Institutes of Health.

Humphrey, D. R., & Tanji, J. (1991). What features of voluntary motor control are encoded in the neuronal discharge of different cortical motor areas. In D. R. Humphrey & H. J. Fruend (Eds.), Motor Control: Concepts and Issues, (pp. 413-414). New York: John Wiley & Sons.

McFarland, D., Lefkowicz, A., & Wolpaw, J. (1997). Design and Operation of an EEG-based Brain-Computer Interface (BCI) with Digital Signal Processing Technology. Behavioral Research Methods, Instruments, and Computers(In Press).

Schwartz, A. (1993). Motor Cortical Activity During Drawing Movements: Population Representation During Sinusoid Tracing. Journal of Neurophysiology, 70(1), 28-36.

Schwartz, A. (1994). Direct Cortical Representation of Drawing. Science, 265, 540-542.

Wolpaw, J., & McFarland, D. (1994). Multichannel EEG-Based Brain-Computer Communication. Electroencephalography and Clinical Neurophysiology, 90, 444-447.

Wolpaw, J., McFarland, D., Neat, G., & Forneris, C. (1991). An EEG-Based Brain-Computer Interface for Cursor Control. Electroencephalography and Neurophysiology, 78, 252-259.

2. b. iv CONTROL OF HAND AND WRIST

Abstract
In the last Quarterly Progress Report, we described a feedforward controller designed to provide independent control of hand grasp and wrist movement in a hand grasp neuroprosthesis. The feedforward controller was successful in generating a tenodesis grasp, and maintaining a constant wrist angle during linear changes in grasp opening and force in the absence of unpredictable disturbances. Furthermore, the addition of an input to the wrist module representing arm orientation was able to eliminate unwanted wrist flexion due to gravity. In this quarter, we concentrated on adding further compensation methods to the feedforward controller to correct for unpredictable disturbances, and also evaluated the effect muscle fatigue has on grasp and wrist parameters.

Purpose
The goal of this project is to design control systems to restore independent voluntary control of wrist position and grasp force in C5 and weak C6 tetraplegic individuals. The proposed method of wrist command control is a model of how control might be achieved at other joints in the upper extremity as well. A weak but voluntarily controlled muscle (a wrist extensor in this case) will provide a command signal to control a stimulated paralyzed synergist, thus effectively amplifying the joint torque generated by the voluntarily controlled muscle. We will design control systems to compensate for interactions between wrist and hand control. These are important control issues for restoring proximal function, where there are interactions between stimulated and voluntarily controlled muscles, and multiple joints must be controlled with multijoint muscles.

Report of progress
A feedforward control system has been developed to integrate control of the hand and wrist in individuals with C5 or C6 level tetraplegia. Evaluation and design was based on computer simulations with a biomechanical model of the arm and hand [Esteki and Mansour 1996; Lemay and Crago 1996]. In this quarter, we evaluated compensation for gravity, which can act to either flex or extend the wrist, depending

on arm orientation, and also evaluated the effect fatigue would have on the feedforward control, since fatigue presents an unpredictable disturbance.

Compensation for Gravity Disturbances

Arm orientation in the gravitational field affects grasp opening and force as well as wrist angle. For example, arm pronation results in gravity acting in the thumb abduction direction. Thus, grasp opening increases compared to when the arm was neutral and gravity was acting in the thumb flexion direction. To correct for gravity disturbances to grasp opening and force, an input representing arm orientation was added to the thumb module. To do this, the thumb module was trained with patterns when the arm was neutral and pronated (as was the case with the wrist module described in the last Quarterly Progress Report). Figure 2.b.iv.1 displays the desired and simulated tenodesis grasp generated with the feedforward controller with arm orientation (as might be derived from an accelerometer) added as an input to the wrist and thumb modules. The feedforward controller successfully generated a tenodesis grasp with minimal error regardless of whether the arm was neutral or pronated. Figure 2.b.iv.2 displays the normalized muscle stimulation levels produced by the feedforward controller when the arm was neutral and pronated. Note that when the arm was pronated, the stimulation of the ECRB increased to prevent wrist flexion. Also, arm pronation resulted in a decrease in EPL stimulation and an increase in FPL/AdP stimulation in order to obtain the desired grasp opening and force.

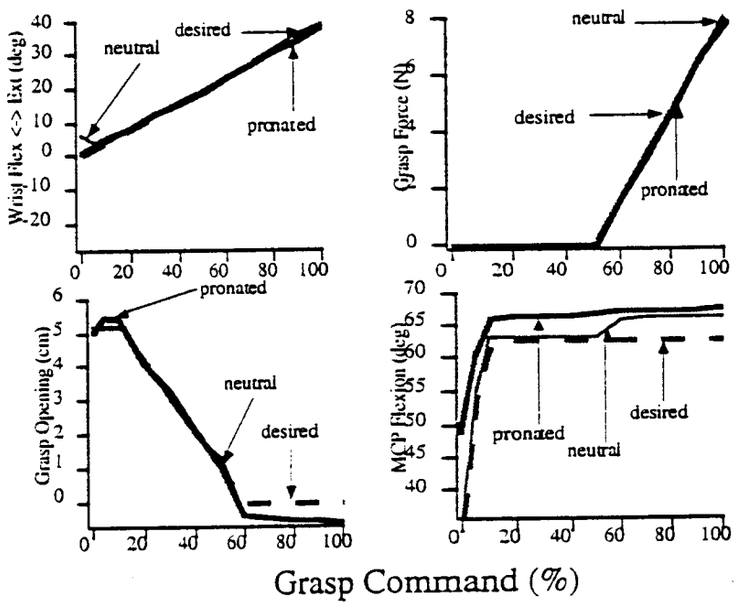

Figure 2.b.iv.1 Desired and simulated tenodesis grasp when arm orientation is an input to wrist and thumb module. Dark dashe lines: desired parameters, light solid lines: simulated parameters when the arm is neutral, dark solid lines: simulated parameters when the arm is pronated.

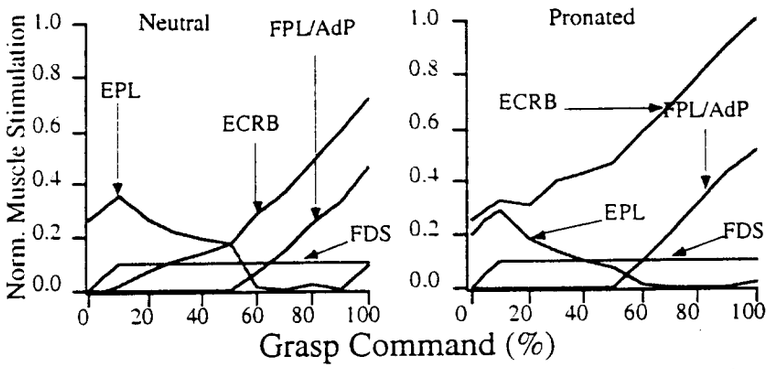

Figure 2.b.iv.2. Normalized muscle stimulation map generated by feedforward controller when the arm was neutral (left hand figure) and pronated (right hand figure). Muscle abbreviations: extensor carpi radialis brevis (ECRB); flexor digitorum superficialis (FDS); extensor pollicis brevis (EPL); flexor pollicis longus (FPL); adductor pollicis (AdP).

Compensation for External Disturbances

In the last Quarterly Progress Report, an external disturbance of 13 N-cm was applied at the wrist to model disturbances due to grasping of an object. Although the error in wrist angle was approximately 20° in the wrist flexion direction, a tenodesis grasp was still possible, and wrist extension beyond 0° was seen once grasp command was greater than 50%. To further correct for external disturbances at the wrist, closed-loop feedback of wrist control was added to the feedforward control scheme (Figure 2.b.iv.3). The feedback controllers that were tested were: (1) proportional controller with a gain of 200, (2) a proportional-derivative (PD) controller with a gain of 200 and a zero of 0.60, and (3) a proportional-integral-derivative (PID) controller with a gain of 30, a zero of 0.60, and a pole of 1.0. The gain of the PID controller was the maximum value that prevented wrist oscillation. To test the addition of feedback control, dynamic simulations were performed, where a 13 N-cm disturbance was imposed at 4.0 seconds.

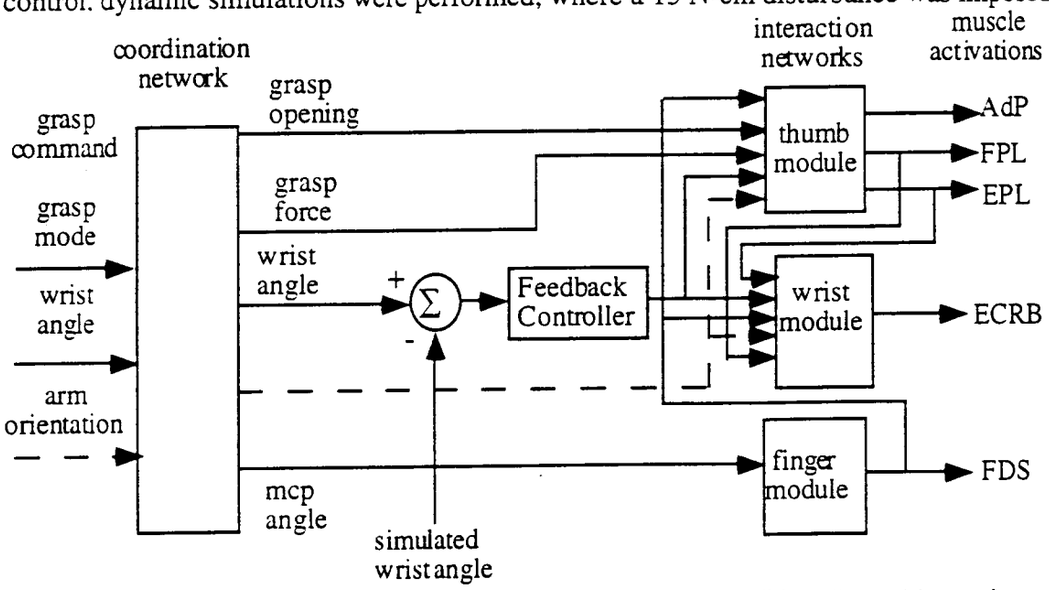

Figure 2.b.iv.3. Design of feedforward controller with the addition of closed-loop wrist control.

Figure 2.b.iv.4 displays the simulated grasp and wrist templates where a constant wrist angle of 15° extension was desired during linear changes in grasp opening and force as a function of time. In these simulations: (1) arm orientation was an input to the wrist and thumb modules, (2) the arm was pronated, and (3) an external disturbance of 13N-cm was applied at 4.0 seconds. The largest error in wrist angle was

when there was no feedback control. The addition of the PD controller reduced the wrist angle error to approximately 15° to 20°, while the proportional controller reduced the error further to 10°. The PID controller eliminated the error in wrist angle; however, there was a little overshoot in wrist angle. In terms of the grasp parameters, errors in grasp opening followed the same pattern as with the wrist angle, while the errors in grasp force were extremely small.

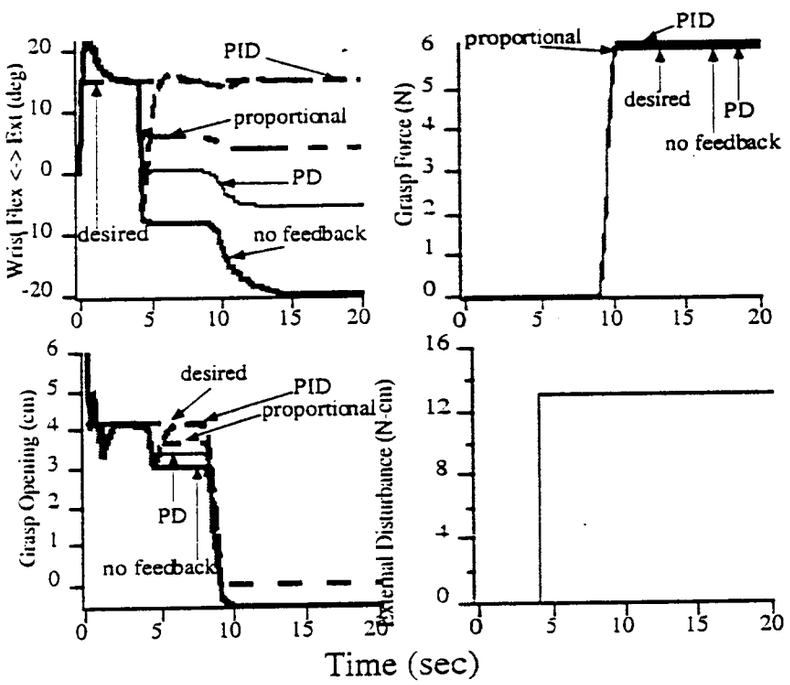

Figure 2.b.iv.4. Simulated grasp and wrist templates with arm pronated and 13 N-cm disturbance added in the wrist flexion direction at 4.0 seconds. Dark dashed line: desired parameters: Dark solid line: parameters with no closed loop wrist control: Dark dash-dot line: proportional wrist controller; Light solid line: PD wrist controller; Dark closer dashed line: PID wrist controller.

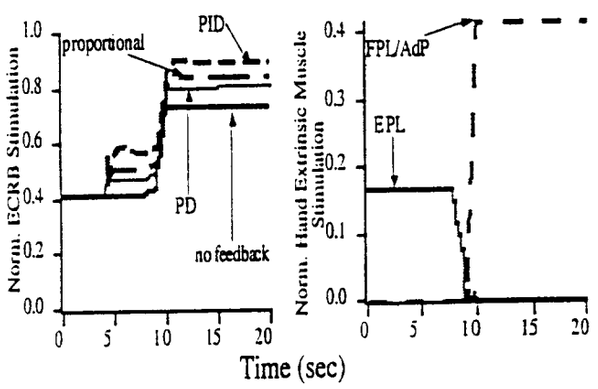

Figure 2.b.iv.5. Normalized stimulus levels of ECRB (left hand figure) and hand extrinsic muscles (right hand figure).

Figure 2.b.iv.5 displays the normalized muscle stimulation levels as a function of time generated by the feedforward/feedback control scheme. Note that since feedback control was not added to the thumb module, the stimulation levels of the EPL and FPL/AdP remained the same regardless of the type of feedback controller tested. In terms of ECRB stimulation, the PID controller increased the simulation level

the most, resulting in the elimination of wrist angle error, as would be expected. Both PD and proportional controllers also increased the stimulation of the ECRB, resulting in the reduction of the wrist angle error.

Muscle Fatigue

To evaluate the effect muscle fatigue has on grasp opening/force and wrist angle, the feedforward controller was used to find the stimulation levels of the hand and wrist muscles for the following conditions: (1) desired grasp force of 2 N and 8 N with a desired wrist angle at 0° and 30° extension, and (2) desired grasp opening of 1 cm with a desired wrist angle at 0° and 30° extension. As with previous simulations, the normalized stimulation levels served as inputs to the biomechanical arm and hand model, but the maximum isometric forces of the ECRB and the hand extrinsic muscles (EPL, FDS, FPL/AdP) were decreased in order to model muscle fatigue. The results of the simulations are displayed in Figure 2.b.iv.6. Muscle fatigue of the ECRB resulted in errors in wrist angle, however, wrist flexion beyond 0° was only seen when the desired grasp force was 8N and the desired wrist angle was 0°. This is because the stimulation of the FPL was high (in order to reach a large grasp force), thus the fatigue of ECRB could not counteract wrist flexion due to stimulation of FPL. When the hand extrinsic muscles were fatigued, a decrease in grasp force was seen, along with an increase in wrist extension. In this instance, the ECRB is over-compensating for the fatigued hand muscles, resulting in additional wrist extension. Fatigue of both hand and wrist muscles resulted in a decrease in grasp force and small changes in wrist angle. The effects of muscle fatigue were more evident with a desired grasp force of 8N since the stimulation of the hand muscles is greater than the stimulation levels needed to reach 2N.

For a desired grasp opening, muscle fatigue had a smaller effect on wrist angle than when a desired grasp force was specified. This is because stimulation of the EPL will still assist wrist extension when the ECRB is fatigued and vise versa, while fatigue of the ECRB when the hand extrinsic flexor muscles were stimulated will result in unwanted wrist flexion. Fatigue of the EPL with and without fatigue of the ECRB produced a smaller grasp opening.

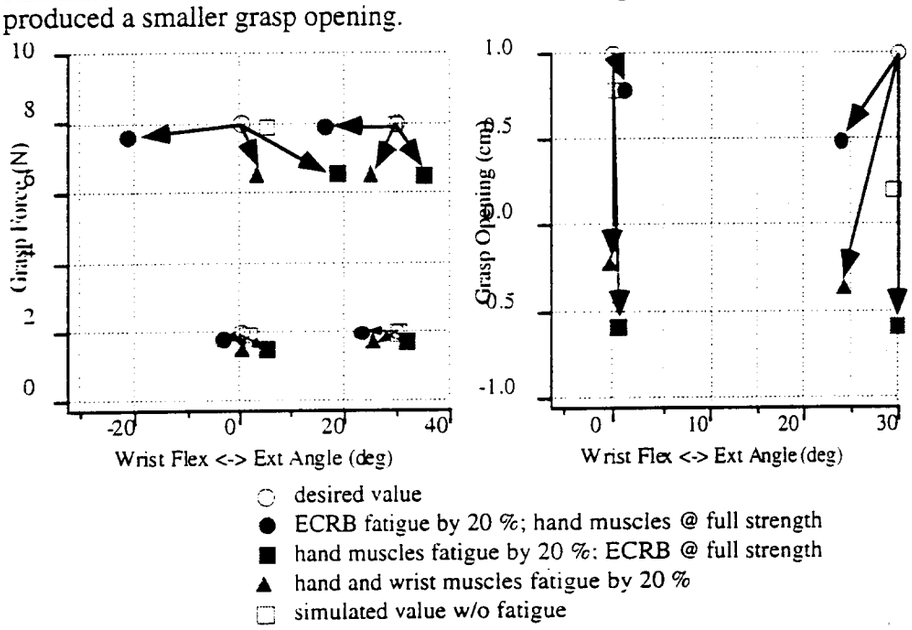

Figure 2.b.iv.6. Simulated grasp force/opening vs. simulated wrist angle for different levels of muscle fatigue. To model muscle fatigue, the maximum isometric muscle force was decreased by 20% for either the ECRB, the hand extrinsic hand muscles, or both. Note that for grasp opening, a negative value represents the thumb flexing below the flexed index finger.

In summary, successful compensation for gravitational disturbances at the wrist and hand was possible by adding an arm orientation input to the wrist and hand modules. Disturbances at the wrist due to external disturbances can be reduced with closed-loop wrist feedback control. However, since feedback control requires external sensors and increases the complexity of the control scheme, it may not be added to the

feedforward controller if successful completion of a grasping tasks is still possible. Muscle fatigue generated errors in hand grasp and wrist angle, but again the effect may not be large enough to prevent grasping of an object or cause slipping of the object.

Plans for next quarter

Plans for the next quarter include attempts at compensating for muscle fatigue, and to begin clinical testing of the feedforward control design.

References

Esteki, A., Mansour, J.M., "A dynamic model of the hand with application in functional neuromuscular stimulation", in press, Annals of Biomedical Engineering 25(5), 1996.

Lemay, M.A., and Crago, P.E., "A dynamic model for simulating movements of the elbow, forearm, and wrist", J. Biomechanics, 29: 1319-1330, 1996.